

**GATING OF REAFFERENCE IN THE EXTERNAL CUNEATE NUCLEUS DURING SELF-  
GENERATED MOVEMENTS IN WAKE BUT NOT SLEEP**

Alexandre Tiriac\*<sup>1,3</sup> & Mark S. Blumberg<sup>1,2,3</sup>

<sup>1</sup> Department of Psychological & Brain Sciences

<sup>2</sup> Department of Biology

<sup>3</sup> The DeLTA Center

The University of Iowa

Iowa City, Iowa 52242 USA

\* Present address:

Department of Molecular & Cell Biology

University of California, Berkeley

142 LSA #3200

Berkeley, CA 94720-3200

Corresponding Author:

Mark S. Blumberg, Ph.D.

E11 Seashore Hall

Department of Psychological & Brain Sciences

The University of Iowa

Iowa City, IA 52242

Email: mark-blumberg@uiowa.edu

Phone: 319-335-2424

## SUMMARY

Nervous systems distinguish between self- and other-generated movements by monitoring discrepancies between planned and performed actions. To do so, corollary discharges are conveyed to sensory areas and gate expected reafference. Such gating is observed in neonatal rats during wake-related movements. In contrast, twitches, which are self-generated movements produced during active (or REM) sleep, differ from wake movements in that they reliably trigger robust neural activity. Accordingly, we hypothesized that the gating actions of corollary discharge are absent during twitching. Here, we identify the external cuneate nucleus (ECN), which processes sensory input from the forelimbs, as a site of movement-dependent sensory gating during wake. Whereas pharmacological disinhibition of the ECN unmasked wake-related reafference, twitch-related reafference was unaffected. This is the first demonstration of a neural comparator that is differentially engaged depending on the kind of movement produced. This mechanism explains how twitches, though self-generated, trigger abundant reafferent activation of sensorimotor circuits in the developing brain.

Animals of diverse vertebrate and invertebrate species distinguish between sensations arising from self-generated movements from those arising from other-generated movements [1,2]. To make this distinction between self and other, motor areas produce copies of motor commands (i.e., corollary discharges) that are directly compared with sensory signals arising from self-generated movements (i.e., reafference; [3,4]). At the level of the neural comparator, reafference is blocked when there are no discrepancies between the corollary discharge and reafferent signals [3,5–7]. As a result, expected reafference arising from voluntary movements is attenuated [8–10], thereby increasing the salience of unexpected reafference [3,11,12].

We previously demonstrated in week-old rats that wake-related movements do not trigger substantial reafference in sensorimotor cortex (SMC). In contrast, sleep-related twitches—which are produced exclusively and abundantly during active (or REM) sleep—trigger robust reafference [13]. We provided converging evidence that twitches, unlike wake movements, are processed by the nervous system *as if* they are unexpected. Accordingly, we hypothesized that the actions of corollary discharge that normally gate reafference arising from wake movements are either absent or inhibited during twitching. If true, there must be a neural structure, located somewhere within the sensorimotor network, that acts as a comparator to specifically gate wake-related reafference.

One possible comparator is the external cuneate nucleus (ECN), which receives primary muscle spindle afferents from forelimb and nuchal muscles and conveys sensory information to downstream structures including the cerebellum, thalamus, and cerebral cortex [14–18]. Moreover, the ECN receives projections from premotor structures that are potential sources of corollary discharge, including the red nucleus [19–21]—which

contributes both to the production of wake movements and twitches in infant rats [22]—and the premotor C3-C4 propriospinal neurons (PNs; [23]), which have been implicated in the conveyance of corollary discharge [23–25]. Corollary discharge from the red nucleus or PNs could contribute to sensory gating in the ECN via known GABAergic and glycinergic inputs to that structure [26–28], perhaps through presynaptic inhibition [9,29].

## RESULTS

### **Twitch-related, but not wake-related, movements trigger reafference in SMC**

We first recorded neural activity in the forelimb region of SMC to confirm that it, like the hindlimb region [13], exhibits state-dependent activity. Unanesthetized and head-fixed postnatal day (P) 8-10 rats cycled spontaneously between sleep and wake with their limbs dangling freely. **Figure 1A** depicts representative spindle bursts (recorded from the local field potential; LFP) and multiunit activity (MUA) in relation to both wake movements and twitches. Spindle bursts and MUA were particularly prominent during periods of twitching and were virtually absent during periods of wake movements. Across all pups, the mean rate of spindle bursts ( $t_5 = 10.2$ ,  $p = 0.0002$ ,  $n = 6$  pups) and unit activity ( $t_7 = 3.9$ ,  $p = 0.006$ ,  $n = 8$  units) was significantly higher during active sleep than during wake (**Fig. 1B**). Moreover, spindle bursts and unit activity were triggered by forelimb twitches with a latency of 100-125 ms (**Fig. 1C**).

### **Twitch-related, but not wake-related, movements trigger reafference in the ECN**

If the ECN is a comparator of reafference and corollary discharge signals, then it should—like the SMC—exhibit state-dependent activity. Therefore, we next recorded from the ECN

in P8-10 rats (**Figure 2A**). As expected, ECN firing rate was higher in response to forelimb twitches than to hindlimb ( $t_8 = 3.5$ ,  $p = 0.008$ ) or nuchal ( $t_{21} = 3.2$ ,  $p = 0.007$ ) twitches (**Figure 2B**); there was no significant difference in ECN firing rate between hindlimb and nuchal twitches ( $t_8 = 1.3$ ,  $p = 0.23$ ). Also as expected given the relative anatomical locations of the ECN and SMC, the latency to twitch-related ECN activity (10-50 ms) was shorter than that observed in SMC (100-125 ms; see **Figure 1C**). Finally, ECN firing rate was state dependent, with greater activity occurring during periods of forelimb twitching than during periods of forelimb wake movement ( $t_{15} = 2.8$ ,  $p = 0.012$ , **Figure 2C**).

It is possible that the inhibition of wake-related reafference was due to a global inhibition of all sensory activity during wake. If so, then stimulation of the ipsilateral forelimb should produce less exafference in the ECN during wake than during sleep. To test for this possibility, we recorded from ECN neurons as the ipsilateral forelimb was stimulated during sleep and wake. As shown in **Figure 2D**, there was no significant effect of behavioral state on ECN activity in response to forelimb stimulation ( $t_5 = 1.2$ ,  $p = 0.286$ ). This result is consistent with our earlier finding in the hindlimb region of SMC [13].

### Disinhibition of the ECN unmasks wake-related reafference

**Figure 3A** depicts our proposed model to explain movement-dependent modulation of reafference in the ECN. To test the model's predictions, we recorded ECN activity before and during combined iontophoretic infusion of GABA<sub>A</sub> (10 mM bicuculline methiodide) and glycine (10 mM strychnine hydrochloride) receptor antagonists or saline (**Figure 3B**;  $n = 5$  pups per group). As predicted, inhibitory blockade of the ECN unmasked reafference in response to forelimb wake movements ( $t_8 = 3.7$ ,  $p = 0.006$ , **Figure 3C**). Moreover, and

again as predicted, inhibitory blockade had no effect on ECN reafference in response to forelimb twitches (**Figure 3D**). As expected, saline infusions had no effect on either wake or sleep reafference.

We next assessed whether inhibitory blockade of the ECN alters motor activity. Blocking GABA and glycine receptors had no effect on the amplitude of wake movements (**Figure 4A**), the frequency of forelimb wake movements (**Figure 4B**), or the frequency of forelimb twitches (**Figure 4C**). Moreover, inhibitory blockade had no effect on tonic neural activity in the ECN (**Figure 4D**), thus providing further evidence that the inhibitory inputs to the ECN function specifically in the context of wake movements.

## DISCUSSION

### The ECN is a neural comparator

To establish that the ECN is a comparator of corollary discharge and reafferent signals, several criteria must be met [30]. First, to be a comparator the ECN must be a sensory structure; in fact, the ECN processes proprioceptive inputs from forelimb and nuchal muscles [14] and recordings from anesthetized cats have demonstrated that the ECN codes, with high fidelity, the stretch on muscle fibers [16]. Second, the ECN must receive motor-related input; in fact, the ECN receives direct and indirect input from premotor areas, including the red nucleus [19–21] and C3-C4 PNs [23]. Third, the ECN should not participate in the production of movement; as shown here, disinhibition of the ECN had no discernible effect on the production of wake movements or twitches (**Figure 4**).

Finally, and most critically, a comparator must gate reafference arising from movements. This was demonstrated here by showing that inhibitory blockade of the ECN

unmasked reafference exclusively during wake movements (**Figure 3C**). Importantly, inhibitory blockade had no effect on the ECN's tonic firing rate (**Figure 4D**), thus demonstrating that inhibitory control of the ECN is not engaged throughout the waking state. Furthermore, when we manually stimulated the forelimbs, ECN activity was evoked similarly during sleep and wake (**Figure 2D**).

### **Possible mechanisms underlying movement-dependent modulation of reafference**

There is no evidence that wake movements and twitches are produced by independent brainstem structures. On the contrary, the red nucleus is involved in the production of both types of movements [22,31]. Therefore, it may be that (a) premotor structures like the red nucleus are state-dependently modulated such that they convey motor copies to the ECN (or an intervening structure) only during wake movements, or (b) the ECN receives motor copies from both types of movements, but state-dependent modulation of the ECN prevents the twitch-related motor copies from engaging the inhibitory mechanism. Indeed, in neonatal rats there are structures, including the noradrenergic locus coeruleus, that could play a state-dependent modulatory role [32]. Regardless of which mechanism turns out to be correct, the fact remains that wake movements and twitches are processed very differently at the level of the ECN.

### **Functional implications**

Experimental disruption of corollary discharge pathways has a negative impact on forelimb reaching [25] and control of eye movements [4]. In this context, the gating of wake-related

reafference within the ECN makes functional sense. But if sensory gating is critical for motor function, why disengage this mechanism during sleep-related twitches?

The absence of sensory gating during sleep raises the possibility that corollary discharge mechanisms interfere with functional processes in which twitches are involved. Indeed, if sensory gating were to occur during active sleep, twitches—which are especially abundant during early development—would trigger little or no reafference. In the context of a developing system that relies heavily on activity-dependent processes [33], the gating of twitch-related reafference would suppress the very activity upon which some of these processes depend. Because reafference is not gated during twitching, it is permitted to sequentially activate interconnected sensorimotor structures—including the ECN (as shown here), red nucleus [22], cerebellum [34,35], thalamus [36,37], sensorimotor cortex [13,37], and hippocampus [38]. Such cascading neural activity provides the opportunity for competitive synaptic interactions that, through such mechanisms as spike-timing-dependent plasticity [39,40], can contribute to the development and refinement of somatotopic organization across the neuraxis.

The very presence of a neural comparator that is differentially engaged in a movement-dependent manner argues both for the importance of sensory gating during wake and its absence during sleep. With regard to the latter, the identification here of a neural mechanism that distinguishes twitches from wake movements reinforces the notion that twitches play a critical role in shaping sensorimotor circuits [41].



## MATERIALS AND METHODS

All experiments were carried out in accordance with the National Institutes of Health Guide for the Care and Use of Laboratory Animals (NIH Publication No. 80-23) and were approved by the Institutional Animal Care and Use Committee of the University of Iowa.

### Subjects

A total of 42 Sprague-Dawley Norway rats (RRID:RGD\_5508397) were used at P8-10. Males and females were used and littermates were always assigned to different experimental groups. Litters were culled to 8 pups within 3 days of birth. Mothers and their litters were housed in standard laboratory cages (48 x 20 x 26 cm). Food and water were available *ad libitum*. All animals were maintained on a 12:12 light-dark schedule with lights on at 0700 h.

### Surgery

*Head-fix preparation.* For all studies, pups were prepared for testing using methods similar to those described previously [22,35,36,42,43]. Under isoflurane anesthesia, bipolar electrodes (50  $\mu$ m diameter; California Fine Wire, Grover Beach, CA) were implanted into the *biceps brachii* muscle of the forelimb, the *extensor digitorum longus* muscle of the hindlimb, and the nuchal muscle. The skin overlying the skull was removed and a custom-built head-fix apparatus was attached to the skull with cyanoacrylate adhesive. A small hole was drilled over the forelimb region of primary sensorimotor cortex (SMC). Forelimb, coordinates in relation to bregma: AP: 1 mm, L: 1.3-1.8 mm, DV: 0.5-0.8 mm) or over the external cuneate nucleus (ECN, coordinates in relation to lambda: AP: -3 mm, L: 1.6 mm,

214 DV: 3.5-4 mm, angle of electrode: 14° directed caudally). After surgery, the pup was  
215 transferred to a humidified incubator maintained at thermoneutrality (35°C) to recover for at  
216 least 1 h, after which it was transferred to a stereotaxic apparatus. The pup's torso was  
217 supported on a narrow platform such that the limbs dangled freely on both sides. The pup  
218 acclimated for at least 1 additional h before recordings began, by which time it was cycling  
219 between periods of sleep and wake.

220

## 221 **Electrophysiological Recordings**

222 The EMG electrodes were connected to a differential amplifier (A-M Systems, Carlsborg,  
223 WA; amplification: 10,000x; filter setting: 300-5000 Hz). To record from forelimb SMC, 16-  
224 channel silicon depth electrodes were used (100 µm vertical separation; NeuroNexus, Ann  
225 Arbor, MI). To record from the ECN, 4-channel silicon depth electrodes were used (50 µm  
226 vertical separation; NeuroNexus, Ann Arbor, MI). Silicon electrodes had impedances  
227 ranging from 1-4 MΩ. To simultaneously perform ECN recordings during iontophoretic  
228 application of GABA and glycine receptor antagonists, multibarrel electrodes were used  
229 with an iontophoretic pump (Kation Scientific, Minneapolis, MN). Electrodes were  
230 connected to a headstage which communicated with a data acquisition system (Tucker-  
231 Davis Technologies, Alachua, FL) that amplified (10,000x) and filtered the signals. All  
232 cortical recordings were obtained using a 0-5000 Hz band-pass filter and all recordings in  
233 ECN were obtained using a 500-5000 Hz band-pass filter. A 60 Hz notch filter was also  
234 used. Neurophysiological and EMG signals were sampled at 25 kHz and 1 kHz,  
235 respectively, using a digital interface and Spike2 software (Cambridge Electronic Design,  
236 Cambridge, UK).

Prior to insertion of the silicon probe into SMC or ECN, the electrode surface was coated with fluorescent DiI (Life Technologies, Carlsbad, CA) for subsequent histological verification of electrode placement. A Ag/AgCl ground electrode (Medwire, Mt. Vernon, NY, 0.25 mm diameter) was placed into the visual cortex ipsilateral to the silicon probe. Brain temperature was monitored using a fine-wire thermocouple (Omega Engineering, Stamford, CT) placed in the visual cortex contralateral to the ground wire. For all experiments, brain temperature was maintained at 36-37 °C.

Electrode position was established when it was possible to reliably evoke neural activity by gentle stimulation of the contralateral (for sensorimotor cortex) or ipsilateral (for ECN) forelimb. Other parts of the body were also stimulated to confirm selectivity. Using procedures similar to those described previously [22,35,36], data acquisition began after local field potentials (LFP) and multiunit activity (MUA) were identified and had stabilized for at least 10 min.

## **Experimental Procedure**

*Spontaneous activity during sleep and wake.* We recorded spontaneous neural activity in cycling unanesthetized infant rats (n = 6 for SMC recordings, n = 14 for ECN recordings). Recording sessions comprised continuous collection of neurophysiological and EMG data for at least 30 min. During acquisition, an experimenter monitored the subject's behavior and digitally marked the occurrence of sleep-related twitching and wake movements in synchrony with the physiological data. For the digital marking of limb movements, we used two sets of markers. One set of digital markers was used for forelimb twitches and wake movements, and another set was used for twitches and wake movements of all limbs. As

described elsewhere [32], myoclonic twitches are phasic, rapid, and independent movements of the limbs and tail against a background of muscle atonia; in contrast, wake movements, which are high-amplitude, coordinated movements occurring against a background of high muscle tone, include locomotion, stretching, and yawning. Finally, the experimenter was always blind to the physiological data when scoring behavior.

*Forelimb stimulation.* In 6 of the 14 animals in which spontaneous sleep-wake activity was recorded in the ECN, the forelimb ipsilateral to the recording site was stimulated using a fine paintbrush over a period of 10 min. The brush was applied to the base of the paw and the limb was flexed at the elbow. The stimulations were performed similarly during sleep and wake. On average, stimulations were repeated every 5-10 s.

*Iontophoretic injections of GABA and glycine receptor antagonists.* In 10 head-fixed P8-10 rats, ECN activity was recorded before and during iontophoretic infusions of GABA<sub>A</sub> (10 mM bicuculline methiodide) and glycine (10 mM strychnine hydrochloride; Sigma-Aldrich, St. Louis, MO) receptor antagonists or saline. Before infusion, 30 min of baseline ECN activity was recorded. During this recording, a -10 nA retaining current was used to ensure that the antagonists did not leak passively into the ECN. After the baseline recording, the current was switched to +50 nA to eject the drugs and another 30 min of ECN activity was recorded. After this recording period, fluorogold was injected with the same current parameter that was used for drug infusion to mark the location of the electrode.

## Histology

At the end of the recording session, the pup was overdosed with sodium pentobarbital (1.5 mg/g) and perfused transcardially with phosphate buffered saline followed by 4% paraformaldehyde. Brains were sectioned at 50  $\mu$ m using a freezing microtome (Leica Microsystems, Buffalo Grove, IL). Recording sites were verified by visualizing the Dil tract or the fluorogold injection at 5-20X magnification using a fluorescent Leica microscope. Tissue slices were then stained using cresyl violet and the location of the recording site was identified.

## **Data Analysis**

*MUA and LFP analysis.* All open channels (initially acquired with 0-5000 Hz band-pass filters) were filtered for multiunit activity (500-5000 Hz). Any channels with units were processed by spike sorting in Spike2 (Cambridge Electronic Design, Cambridge, UK). For LFPs, channels were band-pass filtered (1-40 Hz) to extract spindle bursts. Spindle bursts were defined as comprising at least 3 oscillations, a dominant frequency of 10-15 Hz, and a duration of at least 100 ms [37]. LFP channels were converted using root mean square (RMS) with a time constant of 0.01 s. Five random high-amplitude spindle bursts were averaged and the baseline value of the RMS channel was calculated. The midpoint between those two values was used as a threshold for identification of spindle bursts. A second pass through the data was performed to manually remove any spindle bursts that did not match the requisite criteria. Throughout this process, artifacts in the LFP and MUA signals were identified and manually removed.

*Identification of behavioral state and motor activity.* Sleep and wake periods were defined using methods described previously [32,36]. Briefly, the nuchal EMG signal was

305 dichotomized into periods of high tone (indicative of wake) and atonia (indicative of sleep).  
306 Active sleep was characterized by the occurrence of myoclonic twitches against a  
307 background of muscle atonia [44]. Spikes of EMG activity with amplitudes greater than 3x  
308 baseline were considered twitches.

309 For the identification of forelimb wake movements, the forelimb EMG was rectified  
310 and smoothed (0.01 ms). To be considered a wake movement, a spike in the forelimb  
311 EMG had to be at least 300 ms in duration and had to occur while nuchal muscle tone was  
312 high (indicative of wake). Five random wake movements that met these criteria were  
313 selected and their maximum amplitude was averaged. Using the midpoint between atonia  
314 and max amplitude of wake movements as a threshold, an automatic peak detection was  
315 applied to extract forelimb movements as events. Similar to spindle burst detection, a  
316 second pass through the data was performed to manually remove any wake movements  
317 that did not match the requisite criteria.

318 *Analysis of state dependency.* There were at least 20 bouts of wake and active sleep  
319 for each pup. Across these bouts, the mean rates of spindle burst production and unit  
320 activity were determined. First, for each individual pup, successive bouts of wake and  
321 active sleep were treated as pairs and the Wilcoxon matched-pairs signed-ranks test  
322 (SPSS, IBM, Armonk, NY) was used to test for differences in rates of spindle burst  
323 production and unit activity between the two states. Second, the mean rates of spindle  
324 burst production and unit activity during wake and active sleep were calculated for each  
325 pup and compared within each age group using paired *t* tests.

326 *Event correlations and waveform averages for SMC and ECN activity triggered by*  
327 *twitches.* The relationship between twitches and SMC and ECN activity was assessed as

follows: First, the data for all pups were concatenated into one file. From this file, using twitches as triggers, event correlations (for SMC: 1000-ms windows, 25-ms bins; for ECN: 300-ms windows, 1-ms bins) of unit activity and waveform averages of spindle activity were constructed. We tested statistical significance for both event correlations and waveform averages by jittering twitch events 1000 times within a 500-ms window using the interval jitter parameter settings within PatternJitter [45,46] implemented in Matlab (MathWorks, Natick, MA). We corrected for multiple comparisons using the method of Amarasingham et al. [47]; this method produces upper and lower acceptance bands ( $p \leq .01$ ) for each event correlation and waveform average.

*Stimulus-triggered event correlations and waveform averages.* The 10-min recordings from the forelimb stimulation trials were divided into periods of sleep and wake. Perievent histograms (500-ms windows, 10-ms bins) were constructed using onset of EMG activity produced by forelimb stimulations as the trigger. Average peak firing rate across all stimulations for each behavioral state was determined. Peak firing rate was compared using a paired t test.

*Effects of GABA and glycine receptor antagonists on ECN neural activity.* For each animal in each group, recordings were divided into a pre- and post-infusion period (30 min each). For each time period and for each behavioral state, event correlations (3000-ms windows, 50-ms bins) were generated to correlate MUA activity to ipsilateral forelimb twitches and wake movements. For each event correlation, mean firing rate during quiescence (1-1.5 s preceding motor activity) was calculated. These means were then subtracted from each respective event correlation. For each animal, the event correlation of the pre-infusion time period was subtracted from the event correlation of the post-

infusion time period. The resulting event correlations depicting the change in firing rate ( $\Delta$  firing rate) were then averaged within each experimental group for each behavioral state and standard errors for every bin was calculated. Peak change in firing rate around the expected latency of sensory reafference was then calculated along with standard errors. Experimental groups within each behavioral state were compared using a paired t-test. Expected latency was determined using the raw event correlation for wake (**Figure 3C**) and sleep (**Figure 3D**).

The frequencies of wake movements, twitches, and action potentials across the two time periods were calculated. Statistical significance between time periods was determined using paired t tests. For each of the measurements above, the percent difference between the pre- and post-infusion time periods was also calculated. Statistical significance between experimental groups was determined using an independent samples t test.

Unless otherwise noted, alpha was set at 0.05. Bonferroni corrections were applied when appropriate.

## ACKNOWLEDGMENTS

This work was supported by grants from the National Institutes of Health (R37-HD081168, R01-HD063071) to M.S.B. We thank the members of the Blumberg lab for helpful comments on earlier drafts of the manuscript.

## COMPETING FINANCIAL INTERESTS

The authors declare no competing financial interests.

## REFERENCES

- [1] Crapse TB, Sommer MA. Corollary discharge across the animal kingdom. *Nat Rev Neurosci* 2008;9:587–600. doi:10.1038/nrn2457.
- [2] Sommer MA, Wurtz RH. Brain circuits for the internal monitoring of movements.



- Annu Rev Neurosci 2008;31:317–38. doi:10.1146/annurev.neuro.31.060407.125627.
- [3] Poulet JFA, Hedwig B. The cellular basis of a corollary discharge. *Science* (80- ) 2006;311:518–22. doi:10.1126/science.1120847.
- [4] Sommer MA, Wurtz RH. A pathway in primate brain for internal monitoring of movements. *Science* (80- ) 2002;296:1480–2. doi:10.1126/science.1069590.
- [5] Bell CC. Memory-based expectations in electrosensory systems. *Curr Opin Neurobiol* 2001;11:481–7.
- [6] Brooks JX, Cullen KE. Early vestibular processing does not discriminate active from passive self-motion if there is a discrepancy between predicted and actual proprioceptive feedback. *J Neurophysiol* 2014;111:2465–78. doi:10.1152/jn.00600.2013.
- [7] Bell CC. Sensory coding and corollary discharge effects in mormyrid electric fish. *J Exp Biol* 1989;146:229–53.
- [8] Voss M, Ingram JN, Haggard P, Wolpert DM. Sensorimotor attenuation by central motor command signals in the absence of movement. *Nat Neurosci* 2006;9:26–7. doi:10.1038/nn1592.
- [9] Seki K, Perlmuter SI, Fetz EE. Sensory input to primate spinal cord is presynaptically inhibited during voluntary movement. *Nat Neurosci* 2003;6:1309–16. doi:10.1038/nn1154.
- [10] Haggard P, Whitford B. Supplementary motor area provides an efferent signal for sensory suppression. *Cogn Brain Res* 2004;19:52–8. doi:10.1016/j.cogbrainres.2003.10.018.
- [11] Brooks JX, Carriot J, Cullen KE. Learning to expect the unexpected: rapid updating in primate cerebellum during voluntary self-motion. *Nat Neurosci* 2015;18:1–10. doi:10.1038/nn.4077.
- [12] Brooks JX, Cullen KE. The primate cerebellum selectively encodes unexpected self-motion. *Curr Biol* 2013;23:947–55.
- [13] Tiriac A, Del Rio-Bermudez C, Blumberg MS. Self-generated movements with “unexpected” sensory consequences. *Curr Biol* 2014;24:2136–41. doi:10.1016/j.cub.2014.07.053.
- [14] Campbell SK, Parker TD, Welker W. Somatotopic organization of the external cuneate nucleus in albino rats. *Brain Res* 1974;77:1–23.
- [15] Cooke JD, Larson B, Oscarsson O, Sjölund B. Origin and termination of cuneocerebellar tract. *Exp Brain Res* 1971;13:339–58. doi:10.1007/BF00234336.
- [16] Mackie PD, Morley JW, Rowe MJ. Signalling of static and dynamic features of muscle spindle input by external cuneate neurones in the cat. *J Physiol* 1999;519 Pt 2:559–69.
- [17] Boivie J, Boman K. Termination of a separate (proprioceptive?) cuneothalamic tract from external cuneate nucleus in monkey. *Brain Res* 1981;224:235–46. doi:10.1016/0006-8993(81)90856-8.
- [18] Huang CC, Sugino K, Shima Y, Guo C, Bai S, Mensh BD, et al. Convergence of pontine and proprioceptive streams onto multimodal cerebellar granule cells. *Elife* 2013;2013:1–17. doi:10.7554/eLife.00400.
- [19] Holstege G, Tan J. Projections from the red nucleus and surrounding areas to the brainstem and spinal cord in the cat. An HRP and autoradiographical tracing study. *Behav Brain Res* 1988;28:33–57.

- [20] Edwards SB. The ascending and descending projections of the red nucleus in the cat: an experimental study using an autoradiographic tracing method. *Brain Res* 1972;48:45–63.
- [21] Martin GF, Dom R, Katz S, King JS. The organization of projection neurons in the opossum red nucleus. *Brain Res* 1974;78:17–34.
- [22] Del Rio-Bermudez C, Sokoloff G, Blumberg MS. Sensorimotor processing in the newborn rat red nucleus during active sleep. *J Neurosci* 2015;35:8322–32. doi:10.1523/JNEUROSCI.0564-15.2015.
- [23] Pivetta C, Esposito MS, Sigrist M, Arber S. Motor-circuit communication matrix from spinal cord to brainstem neurons revealed by developmental origin. *Cell* 2014;156:537–48. doi:10.1016/j.cell.2013.12.014.
- [24] Alstermark B, Isa T, Pettersson LG, Sasaki S. The C3-C4 propriospinal system in the cat and monkey: A spinal pre-motoneuronal centre for voluntary motor control. *Acta Physiol* 2007;189:123–40. doi:10.1111/j.1748-1716.2006.01655.x.
- [25] Azim E, Jiang J, Alstermark B, Jessell TM. Skilled reaching relies on a V2a propriospinal internal copy circuit. *Nature* 2014;508:357–63. doi:10.1038/nature13021.
- [26] Galindo A, Krnjević K, Schwartz S. Micro-iontophoretic studies on neurones in the cuneate nucleus. *J Physiol* 1967;192:359–77.
- [27] Heino R, Westman J. Quantitative analysis of the feline dorsal column nuclei and their GABAergic and non-GABAergic neurons. *Anat Embryol (Berl)* 1991;184:181–93. doi:10.1007/BF01673255.
- [28] Sato K, Zhang JH, Saika T, Sato M, Tada K, Tohyama M. Localization of glycine receptor alpha 1 subunit mRNA-containing neurons in the rat brain: an analysis using in situ hybridization histochemistry. *Neuroscience* 1991;43:381–95. doi:0306-4522(91)90302-5 [pii].
- [29] Andersen P, Eccles JC, Schmidt RF, Yokota T. Depolarization of presynaptic fibers in the cuneate nucleus. *J Neurophysiol* 1964;27:92–106.
- [30] Poulet JFA, Hedwig B. New insights into corollary discharges mediated by identified neural pathways. *Trends Neurosci* 2007;30:14–21. doi:10.1016/j.tins.2006.11.005.
- [31] Gassel MM, Marchiafava PL, Pompeiano O. Rubrospinal influences during desynchronized sleep. *Nature* 1966;209:1218–20.
- [32] Karlsson KAE, Gall AJ, Mohns EJ, Seelke AMH, Blumberg MS. The neural substrates of infant sleep in rats. *PLoS Biol* 2005;3:0891–901. doi:10.1371/journal.pbio.0030143.
- [33] Kirkby LA, Sack GS, Firl A, Feller MB. A role for correlated spontaneous activity in the assembly of neural circuits. *Neuron* 2013;80:1129–44. doi:10.1016/j.neuron.2013.10.030.
- [34] Sokoloff G, Uitermarkt BD, Blumberg MS. REM sleep twitches rouse nascent cerebellar circuits: Implications for sensorimotor development. *Dev Neurobiol* 2015;75:1140–53. doi:10.1002/dneu.22177.
- [35] Sokoloff G, Plumeau AM, Mukherjee D, Blumberg MS. Twitch-related and rhythmic activation of the developing cerebellar cortex. *J Neurophysiol* 2015;114:1746–56. doi:10.1152/jn.00284.2015.
- [36] Tiriack A, Uitermarkt BD, Fanning AS, Sokoloff G, Blumberg MS. Rapid whisker movements in sleeping newborn rats. *Curr Biol* 2012;22:2075–80.

- [37] Khazipov R, Sirota A, Leinekugel X, Holmes GL, Ben-Ari Y, Buzsáki G. Early motor activity drives spindle bursts in the developing somatosensory cortex. *Nature* 2004;432:758–61. doi:10.1038/nature03132.
- [38] Mohs EJ, Blumberg MS. Neocortical activation of the hippocampus during sleep in infant rats. *J Neurosci* 2010;30:3438–49. doi:10.1523/JNEUROSCI.4832-09.2010.
- [39] Feldman D. The spike-timing dependence of plasticity. *Neuron* 2012;75:556–71. doi:10.1016/j.neuron.2012.08.001.
- [40] Song S, Abbott LF. Cortical development and remapping through spike timing dependent plasticity. *Neuron* 2001;32:339–50.
- [41] Blumberg MS, Marques HG, Iida F. Twitching in sensorimotor development from sleeping rats to robots. *Curr Biol* 2013;23:R532–7. doi:10.1016/j.cub.2013.04.075.
- [42] Blumberg MS, Coleman CM, Gerth AI, McMurray B. Spatiotemporal structure of REM sleep twitching reveals developmental origins of motor synergies. *Curr Biol* 2013;23:2100–9. doi:10.1016/j.cub.2013.08.055.
- [43] Blumberg MS, Sokoloff G, Tiriac A, Del Rio-Bermudez C. A valuable and promising method for recording brain activity in behaving newborn rodents. *Dev Psychobiol* 2015;57:506–17. doi:10.1002/dev.21305.
- [44] Seelke AMH, Blumberg MS. The microstructure of active and quiet sleep as cortical delta activity emerges in infant rats. *Sleep* 2008;31:691–9.
- [45] Amarasingham A, Harrison MT, Hatsopoulos NG, Geman S. Conditional modeling and the jitter method of spike resampling. *J Neurophysiol* 2012;107:517–31. doi:10.1152/jn.00633.2011.
- [46] Harrison MT, Geman S. A rate and history-preserving resampling algorithm for neural spike trains. *Neural Comput* 2009;21:1244–58. doi:10.1162/neco.2008.03-08-730.
- [47] Amarasingham A, Harrison MT, Hatsopoulos NG, Geman S. Conditional modeling and the jitter method of spike re-sampling: Supplement. *J Neurophysiol* 2011;arXiv. Ava. doi:10.1152/jn.00633.2011.

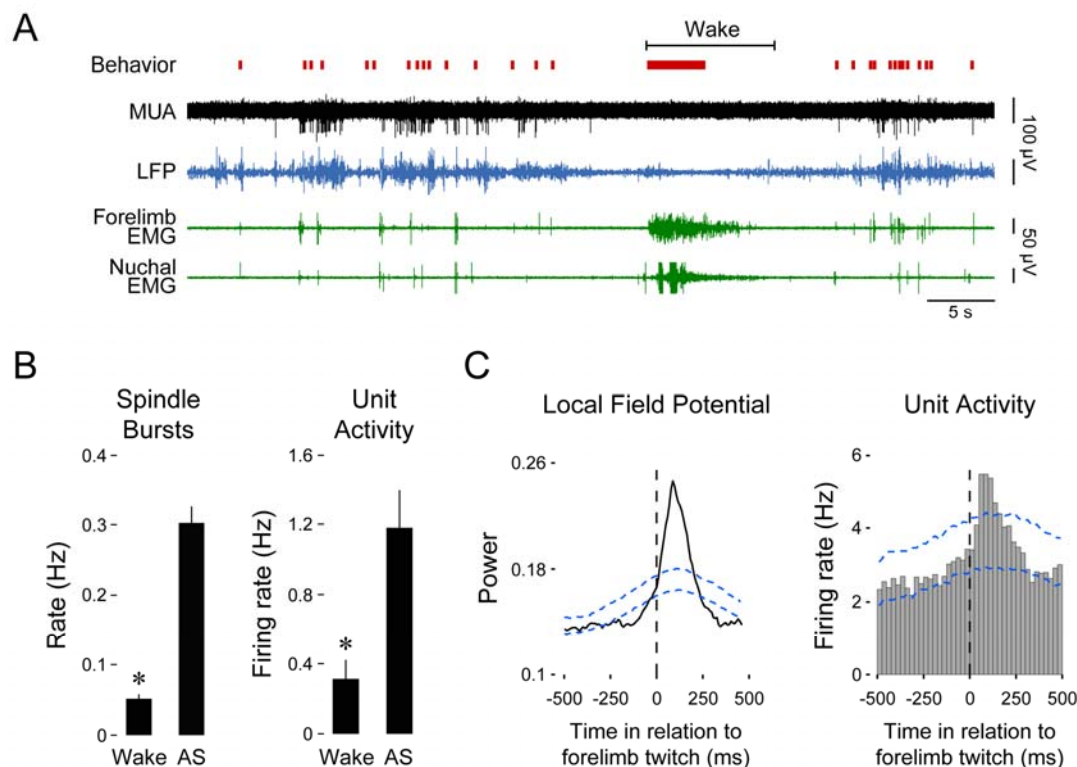
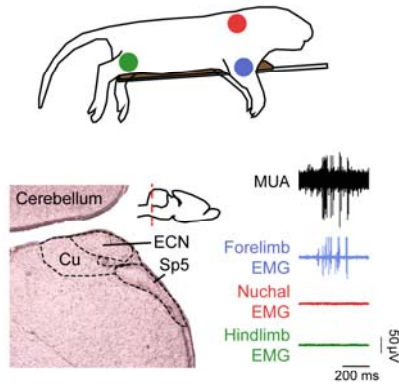
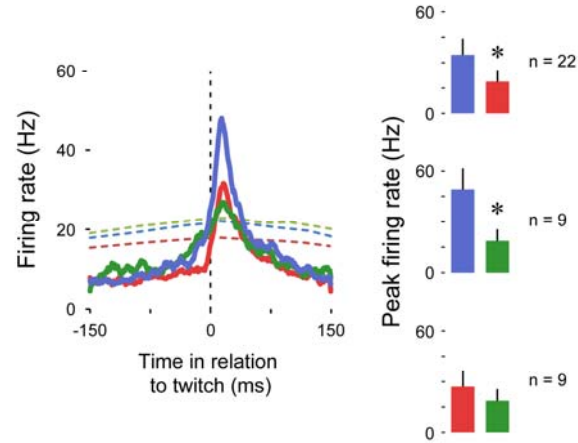


**Figure 1. Forelimb twitches, but not wake movements, trigger neural activity in forelimb sensorimotor cortex.** (A) Representative data depicting sleep and wake behavior, MUA, LFP, and forelimb and nuchal EMG during spontaneous sleep-wake cycling. Red tick marks denote forelimb twitches and red horizontal bars denote forelimb wake movements as scored by the experimenter. (B) Mean (+SEM) rate of spindle burst ( $n = 6$  pups) and unit activity ( $n = 8$  units) during periods of wake and active sleep (AS). The mean rate of spindle bursts and unit activity was significantly higher during active sleep than during wake. \* significant difference from active sleep,  $p < 0.01$ . (C) Waveform average and event correlation for LFP power and unit activity, respectively, in relation to forelimb twitches (2413 and 2943 twitches, respectively). The blue dashed lines denote upper and lower acceptance bands ( $p \leq 0.01$ ).

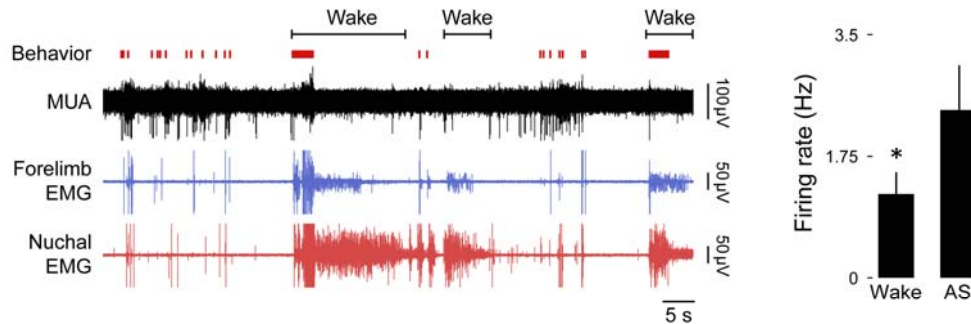
## A. Method



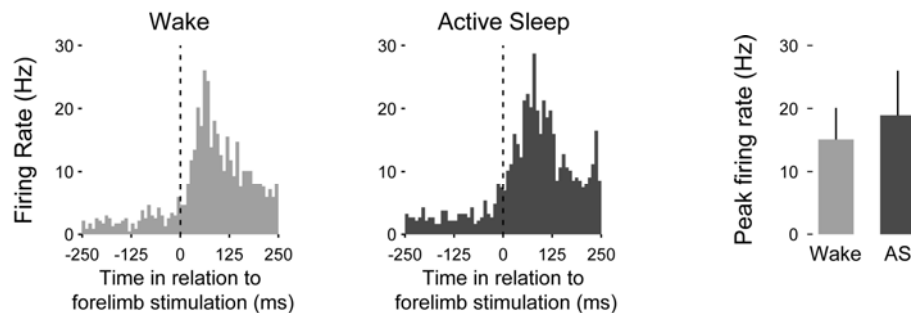
## B. Twitch-dependent activity



## C. Spontaneous Activity



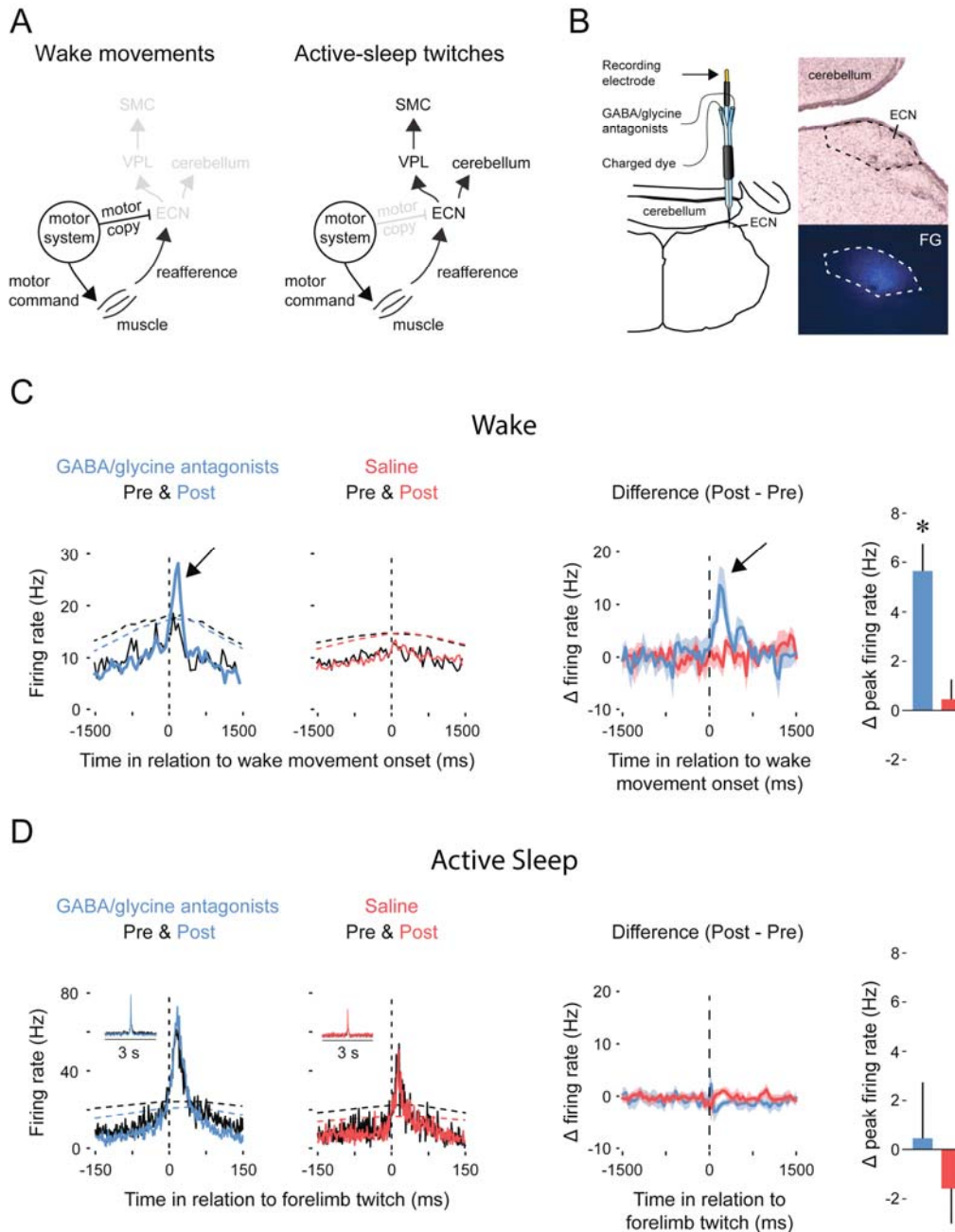
## D. Evoked Activity



521

522 **Figure 2. The ECN exhibits wake-dependent inhibition of sensory reafference.** (A)  
 523 Top: For all ECN recordings, P8-10 rats were instrumented with forelimb (blue) and nuchal  
 524 (red) EMGs (n = 22). A subset of these rats also had a hindlimb (green) EMG (n = 9). The  
 525 torso was supported by a platform and the limbs dangled freely. Bottom left: Coronal brain  
 526 section depicting the anatomical location of the ECN in the hindbrain (inset; red dashed  
 527 line depicts AP position of the coronal section). Bottom right: Sample record of a burst of  
 528 ECN reafference in response to forelimb twitches. (B) Left: Event correlations for unit  
 529 activity in relation to forelimb (blue, n = 8146 twitches), nuchal (red, n = 9603 twitches),

and hindlimb (green,  $n = 1243$  twitches) twitches. The colored dashed lines denote upper acceptance bands ( $p \leq 0.01$ ) for the event correlations. Right: Pairwise comparisons of mean ( $\pm$ SEM) peaks in unit activity (Hz) in response to forelimb, nuchal, and hindlimb twitches. Comparisons are between forelimb and nuchal muscles (top), forelimb and hindlimb muscles (middle), and nuchal and hindlimb muscles (bottom). (C) Left: Representative data depicting sleep and wake behavior, MUA, and forelimb and nuchal EMG during spontaneous sleep-wake cycling. Red tick marks denote forelimb twitches, and red horizontal bars denote forelimb wake movements as scored by the experimenter. Right: Mean ( $\pm$ SEM) unit activity ( $n = 16$ ) during wake and active sleep (AS) periods. \* significant difference from active sleep,  $p < 0.05$ . (D) Left: Event correlations for evoked unit activity in response to forelimb stimulations performed during active sleep ( $n = 188$  stimulations) and wake ( $n = 238$  stimulations) across 6 ECN units in 6 pups. Right: Mean ( $\pm$ SEM) peak unit activity ( $n = 6$ ) derived from event correlations during wake and active sleep.



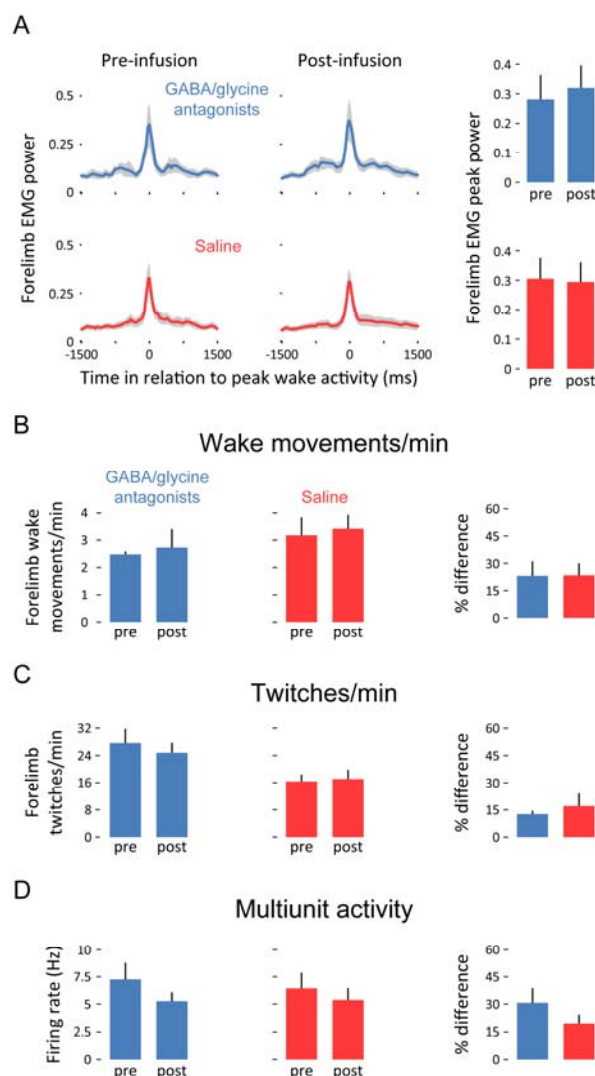
554

555 **Figure 3. Pharmacological blockade of GABA and glycine receptors in the ECN**  
 556 **specifically unmasks refference from self-generated wake movements.** (A)  
 557 Proposed circuitry depicting how refference arising from self-generated movements is  
 558 modulated at the level of the ECN. Left: During wake, ECN inputs arising from motor areas  
 559 convey a corollary discharge (i.e., motor copy) signal that gates expected refference,  
 560 resulting in decreased activity in the ECN and downstream sensory areas. Right: During  
 561 active sleep, the motor copy is absent or inhibited and, therefore, ECN inputs arising from  
 562 motor areas do not gate refference, resulting in activity in the ECN and downstream

sensory areas. VPL: ventral posterolateral nucleus of thalamus; SMC: primary sensorimotor cortex. (B) ECN recordings were performed using multibarrel electrodes filled with either with a GABA<sub>A</sub> antagonist (10 mM bicuculline methiodide) and a glycine antagonist (10 mM strychnine hydrochloride) or saline. For all animals, a separate barrel of the electrode was filled with fluorogold (FG) to mark the location of the recording and estimate the spread of the drug (image at bottom right). (C) Left: Event correlations for unit activity in relation to the onset of forelimb wake movements in animals in the GABA/glycine (blue) or saline (red) groups before (Pre) and after (Post) infusion. Data are pooled across all pups. The dashed lines denote upper acceptance bands ( $p \leq 0.01$ ) for the event correlations. Right: Event correlations depicting the changes in unit activity between the pre-infusion and post-infusion periods for the GABA/glycine (blue) and saline (red) groups. Color-coded shaded regions denote  $\pm$ SEM. Histograms depict mean ( $\pm$ SEM) peak changes in unit activity.  $n = 5$  per group. \* significant difference from saline,  $p < 0.05$ . (D) Same as in (C) but during active sleep; event correlations are triggered on forelimb twitches.



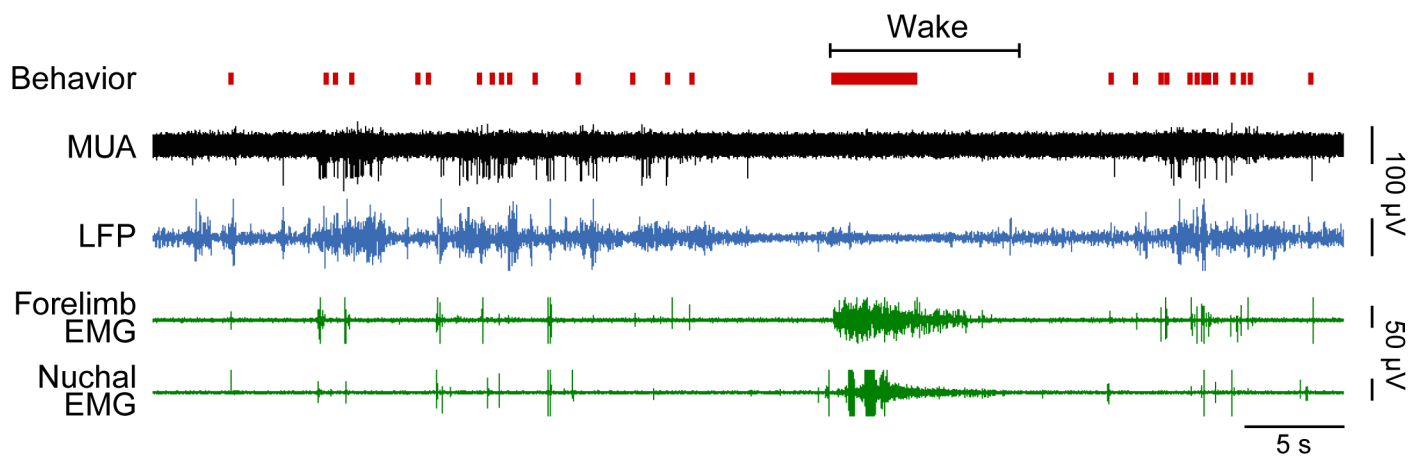
593



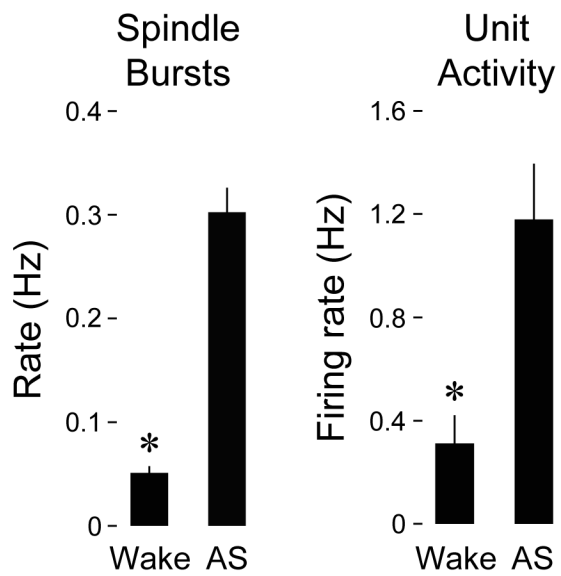
594

595 **Figure 4. Pharmacological blockade of GABA and glycine receptors in the ECN**  
 596 **does not affect forelimb motor activity or tonic ECN unit activity.** (A) Waveform  
 597 averages (3-s time windows) depicting forelimb EMG power in relation to peak forelimb  
 598 wake activity before and after infusion of GABA and glycine receptor antagonists (blue)  
 599 or saline (red). Shaded regions denote  $\pm$ SEM. At right, mean ( $\pm$ SEM) forelimb EMG  
 600 peak power derived from waveform averages. (B) Top row: Mean ( $\pm$ SEM) forelimb wake  
 601 movements/min before and after infusion of GABA and glycine receptor antagonists  
 602 (blue) or saline (red). At right, mean ( $\pm$ SEM) percent difference (pre vs. post) in forelimb  
 603 wake movements/min for both experimental groups. (C) and (D): Same as in (B) but for  
 604 twitches/min and unit activity (in Hz), respectively. None of the differences in this figure  
 605 are significant.

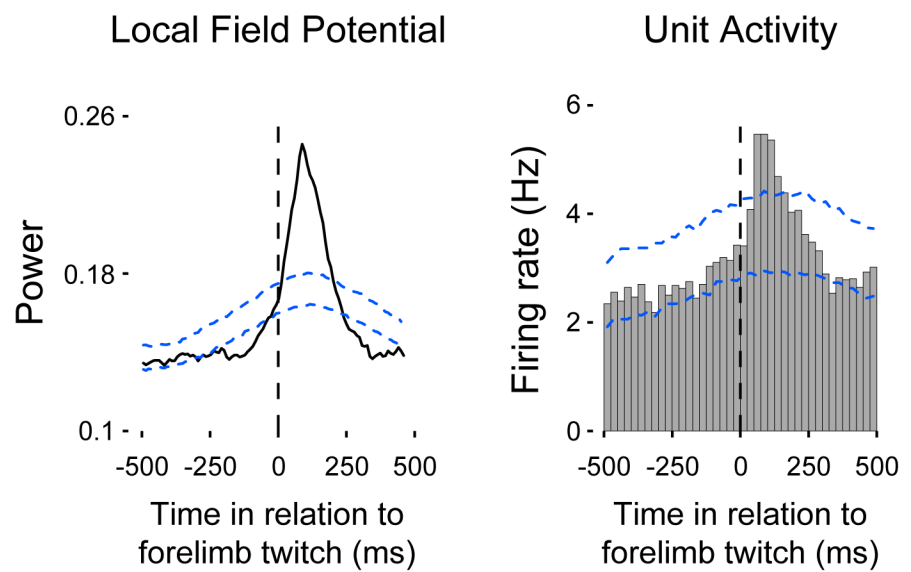
**A**



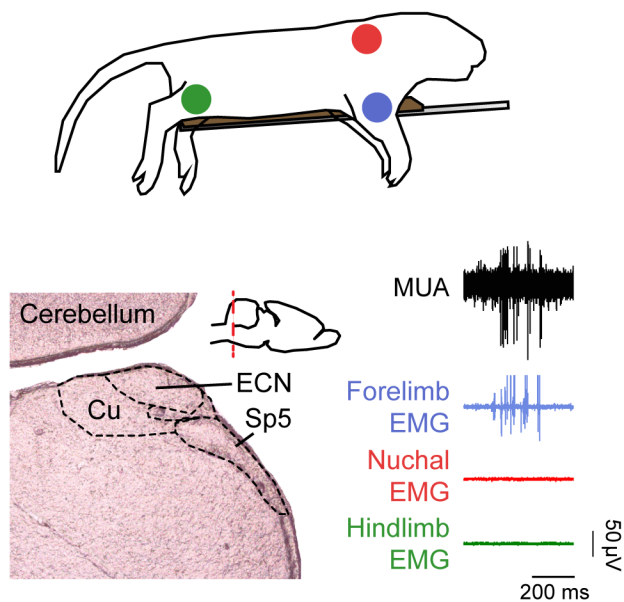
**B**



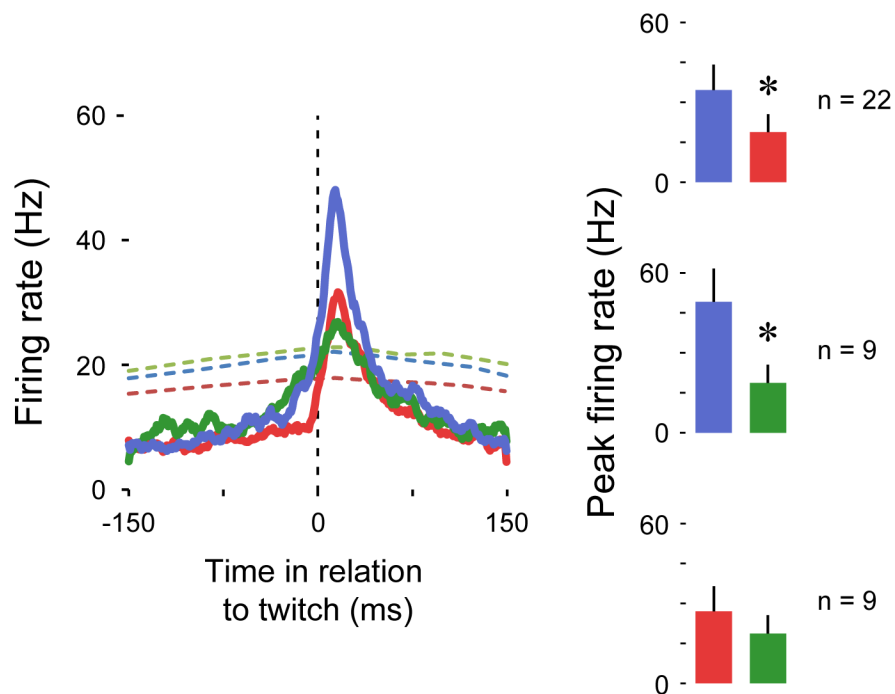
**C**



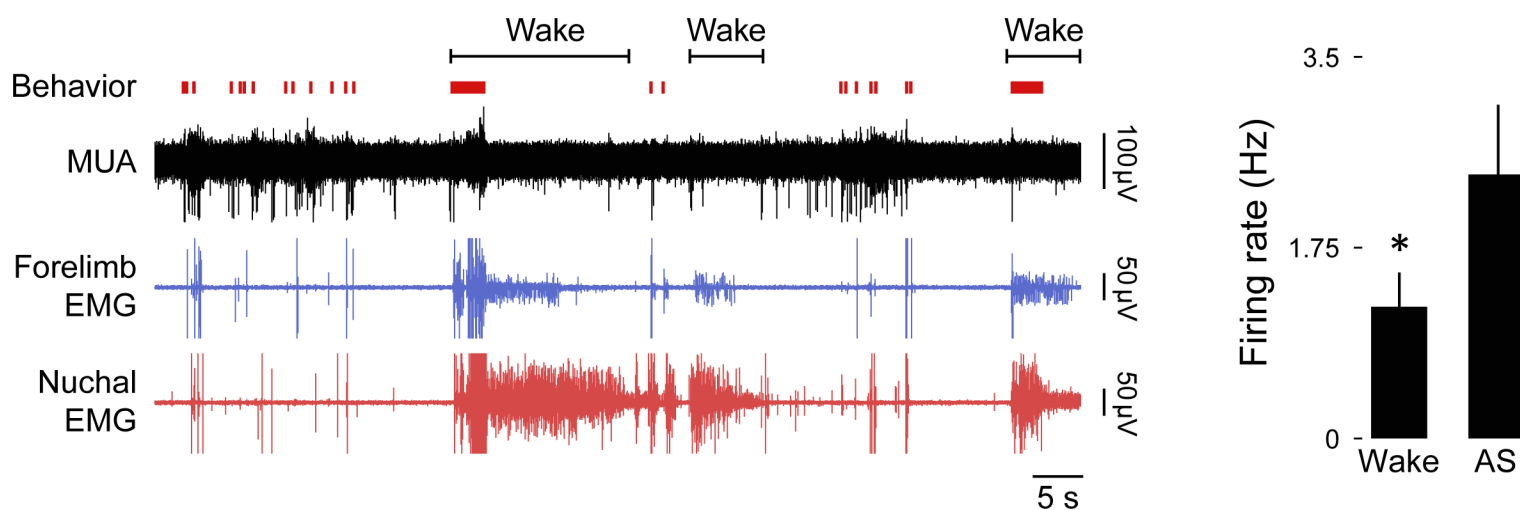
## A. Method



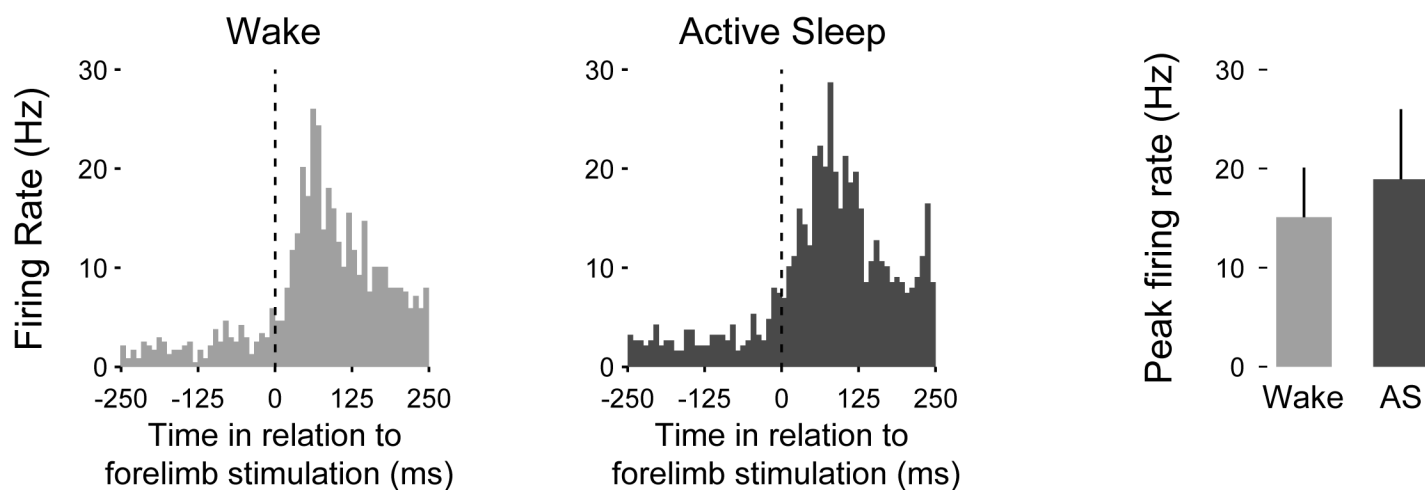
## B. Twitch-dependent activity



## C. Spontaneous Activity

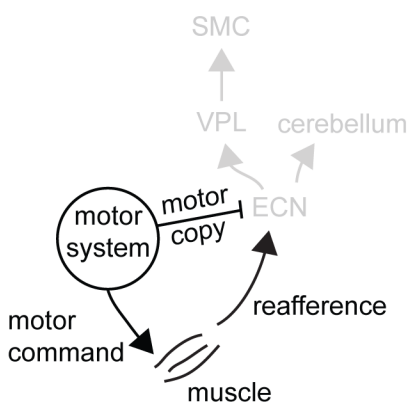


## D. Evoked Activity

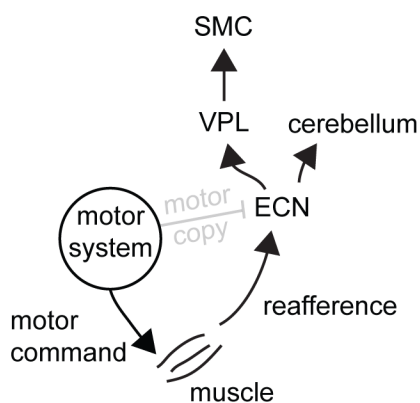


A

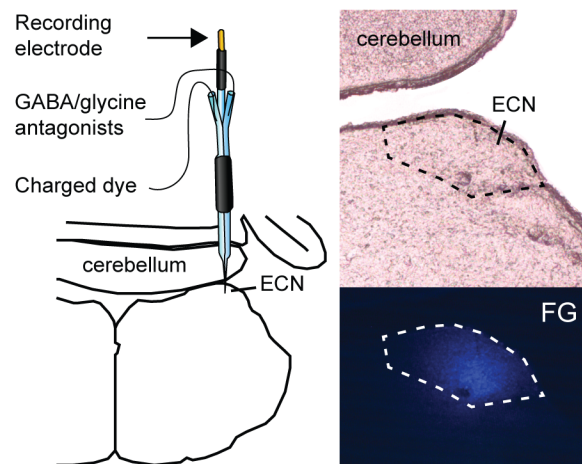
## Wake movements



## Active-sleep twitches

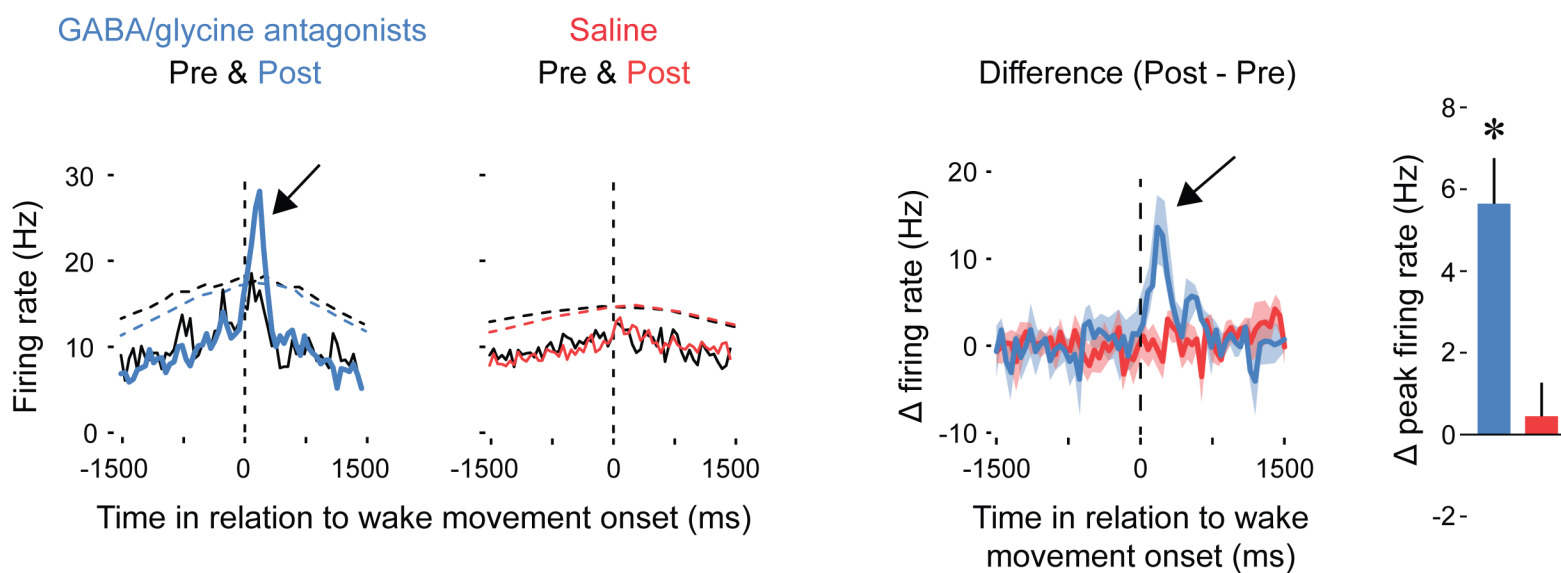


B



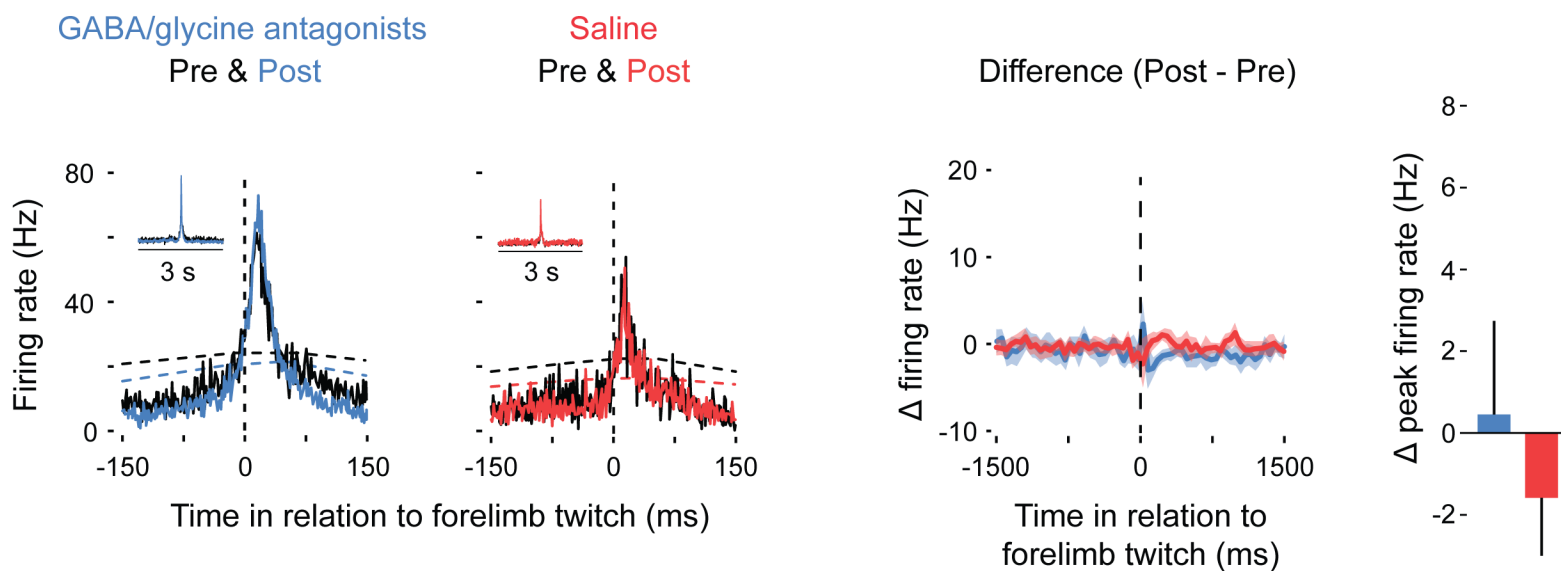
C

## Wake

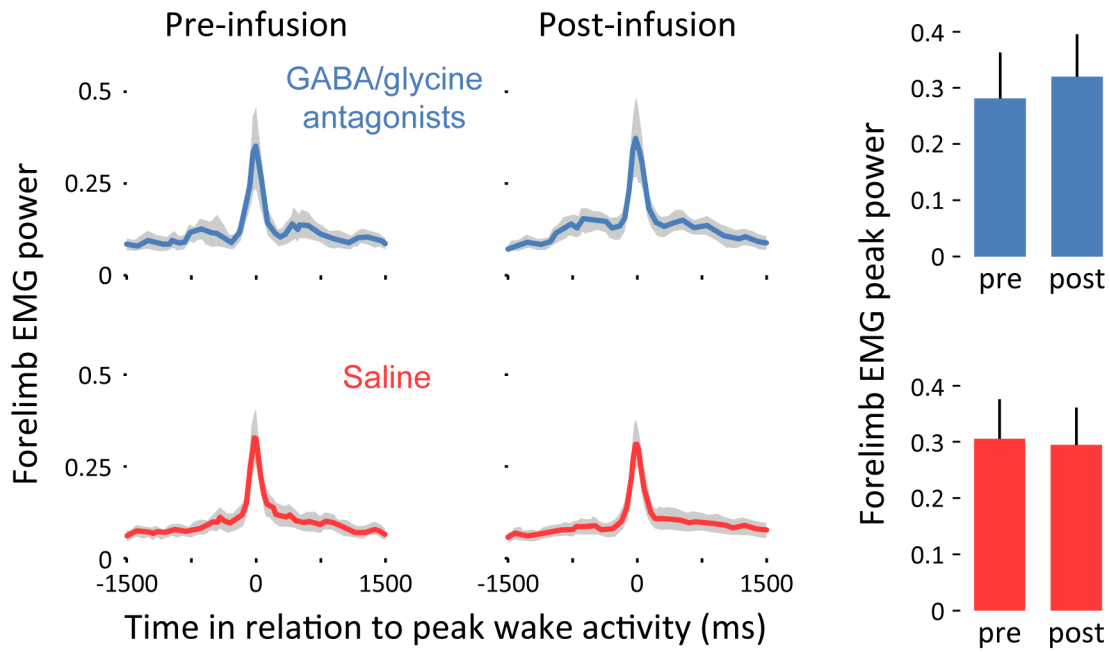


D

## Active Sleep

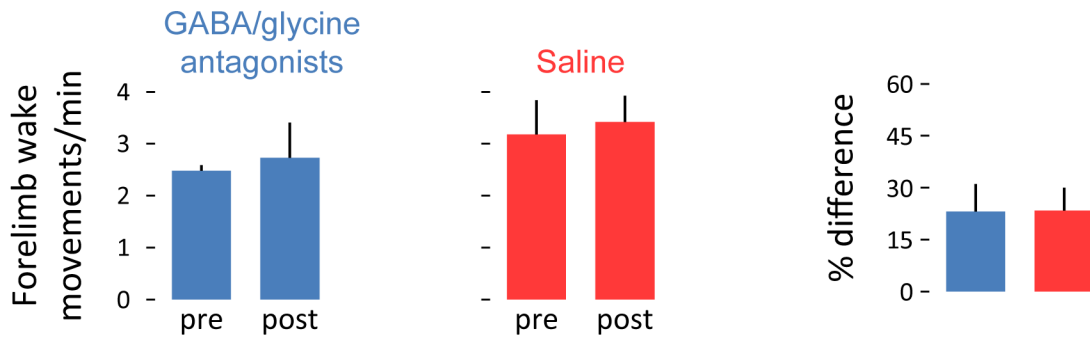


A



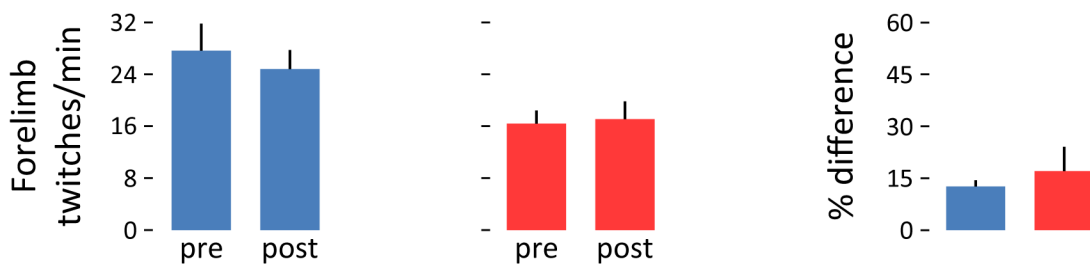
B

## Wake movements/min



C

## Twitches/min



D

## Multiunit activity

